The Relationship between naloxone-induced cortisol and mu opioid receptor availability in mesolimbic structures is disrupted in alcohol dependent subjects

Gary S. Wand[1,2], **Elise M. Weerts**[2], **Hiroto Kuwabara**[3], **Dean F. Wong**[2,3,4,5], **Xiaoqiang Xu**[1], and **Mary E. McCaul**[2,1]

[1]Department of Medicine, The Johns Hopkins University School of Medicine Baltimore, Maryland 21205

[2]Department of Psychiatry and Behavioral Sciences, The Johns Hopkins University School of Medicine Baltimore, Maryland 21205

[3]Department of Radiology, The Johns Hopkins University School of Medicine Baltimore, Maryland 21205

[4]Department of Neuroscience, The Johns Hopkins University School of Medicine Baltimore, Maryland 21205

[5]Department of Environmental Health Sciences, The Johns Hopkins University School of Medicine Baltimore, Maryland 21205

Abstract

The mu opioid receptor system is altered in alcohol dependent (AD) subjects. Cortisol responses to opioid receptor antagonists are assumed to impart information about opioid receptor activity. In the present study we examined naloxone-induced cortisol responses in 18 healthy control (HC) and 25 recently detoxified AD subjects and then correlated the cortisol response with mu opioid receptor availability across 15 brain regions using positron emission tomography (PET) and the mu opioid receptor selective ligand [11C] Carfentanil (CFN). On average the AD subjects required twice the dose of naloxone to induce a peak cortisol response compared to the HC subjects. Using the rising slope of the cortisol curve (placebo to peak) as a metric we then went on to examine the relationship between cortisol responses to naloxone and [11C]CFN BP_{ND}. There were significant negative relationships between cortisol and [11C]CFN binding potential (BP_{ND}) in multiple brain

regions of HC subjects. However, cortisol responses did not correlate with $[^{11}C]$CFN BP_{ND} across any brain region in AD subjects. In summary, naloxone imparts information about individual differences in mu opioid receptor availability throughout the mesolimbic system in healthy individuals. However pathways governing the relationship between naloxone-induced cortisol and mu opioid receptor availability are disrupted during early abstinence in AD subjects.

Keywords

mu opioid receptors; naloxone; PET imaging; HPA axis; cortisol; alcoholism

Introduction

There are several lines of evidence that implicate central nervous system (CNS) opioid systems in the development and maintenance of alcohol dependence (Oswald and Wand, 2004). The targeted disruption of mu opioid receptors in mice reduces alcohol consumption (Hall et al, 2001). Moreover opioid receptor antagonist administration decreases alcohol consumption in rodents, primates and humans (Kranzler and Edenberg, 2010, O'Malley and Froehlich, 2003). In human laboratory studies, naltrexone administration reduced craving and positive reinforcing stimulant effects and increased sedative effects of alcohol compared with placebo administration (McCaul et al 2000/2001; Sinha and O'Malley, 1999; Swift et al, 1994).

A second line of evidence derives from neurobiological studies which indicate that alcohol exposure alters opioid peptides and their receptors. For example, acute alcohol administration increases beta-endorphin and enkephalin gene expression in specific brain regions (Gianoulakis, 1990; Leriche and Mendez, 2010; Li & Froehlich, 1996;) whereas chronic alcohol exposure generally decreases beta-endorphin levels in several brain regions (Chen et al, 2004; Genazzani et al 1982; Sarkar et al, 2007). Alcohol administration also can alter opioid receptor density and/or affinity (Mendez et al, 2005). Recent human PET imaging studies using the mu opioid receptor selective ligand $[^{11}C]$ Carfentanil (CFN) have shown elevated mu opioid receptor availability in AD subjects compared to HC (W Heinz et al, 2005; Weerts et al, 2011).

A third line of evidence is derived from naloxone challenge studies. The non-selective opioid receptor antagonist naloxone has been utilized to provide qualitative information on the status of the endogenous opioid system (Wand et al, 1998). Activation of the HPA axis by naloxone occurs through the blockade of opioid inhibitory tone directed at the hypothalamic regulators of ACTH secretion. Studies using opioid receptor antagonists have presumed to identify differences in opioid activity due to alcohol dependence as well as that conferred by a family history of alcoholism (Adinoff et al, 2005; Wand et al, 1998; Wand et al, 1999). This assumption was recently given more credence by two reports comparing PET measurement of mu and delta opioid receptor availability with cortisol responses to naloxone in healthy subjects. The analysis demonstrated that cortisol responses to a naloxone challenge in healthy subjects were negatively correlated with mu and delta opioid receptor availability in certain mesolimbic regions (Wand et al, 2011; Wand et al, In Press). In the previous studies we compared the relationship of mu and delta opioid receptor binding potential with area under the cortisol curve (AUC). For the current study we wanted to extend our findings in two ways. First we tested three additional cortisol metrics to correlate with mu opioid receptor availability: peak response, dose at peak response and the rising slope of the cortisol curve. This was done to see if we could identify a more robust cortisol metric that would correlate more strongly with receptor availability and in more brain regions than the AUC metric. Second, using the new cortisol metrics we determined

the utility of a naloxone challenge procedure to investigate mu opioid receptor availability in AD subjects. We hypothesized that the negative correlation between naloxone-induced cortisol and mu opioid receptor availability previously identified in HC subjects would be disrupted in AD subjects. This hypothesis was also supported by our recent findings that the relationship between naloxone-induced cortisol and delta opioid receptor availability in mesolimbic structures is disrupted in AD subjects (Wand et al, In Press).

Methods

Subjects

Subjects were 18 (11 male, 7 female) HC subjects and 25 (18 male, 7 female) current AD subjects who completed an inpatient study which included PET imaging and a naloxone challenge procedure (see Weerts et al, 2008; Wand et al. 2011 and described briefly below. Subjects were mostly Caucasian (60%) and matched for age (mean 47.1 ± 8.8 SD yrs for controls and 43.8 ± 7.4 for AD). AD subjects were active drinking at NIAAA-defined hazardous levels (mean 12.4 ± 6.5 SD drinks per day, and 5.5 ± 1.4 SD days per week) as determined by completion of a 90-day Time Line Follow Back (Sobel and Sobel, 1992), and met DSM-IV criteria for alcohol dependence based on the Semi-Structured Assessment of the Genetics of Alcoholism (Bucholz et al, 1994); aged matched HC subjects were light social drinkers who drank below NIAAA recommended guidelines (mean 1.5 ± 1.0 SD drinks per day, and 0.9 ± 1.5 SD drinks per week) and did not meet current or lifetime DSM-IV criteria for either alcohol abuse or dependence. Alcohol Dependence Scores (mean + SD) were $19.6 + 6.7$ for AD subjects and $0.1 + 0.3$ for HCs. Exclusionary criteria for all subjects included: 1) current or lifetime DSM-IV diagnostic criteria for any other Axis I disorder, including other drug abuse/dependence (except nicotine), 2) a significant and active medical illness, 3) positive toxicology at assessment or session days, 4) abnormal CBC or liver enzyme > 2X normal range, 5) pregnancy or taking hormonal birth control, 6) maternal drinking during pregnancy. To avoid use of medications to treat alcohol withdrawal symptoms, AD subjects were excluded for history of seizures or the administration of medication to treat withdrawal symptoms occurring in previous detoxifications. Complete demographic data has been published previously (Weerts et al., 2011). Preceding admission to the CRU, magnetic resonance imaging (MRI) was completed to permit within-subject localization of CNS regions (Meltzer et al, 1990). Research was approved by the Johns Hopkins University Internal Review Board and all subjects provided informed consent.

Inpatient Procedures following admission to Clinical Research Unit (CRU)

AD subjects were admitted to the CRU under an inpatient protocol for medically supervised alcohol withdrawal. On day 5 of the CRU stay, AD subjects underwent PET imaging. The next day the naloxone procedure was completed. These subjects remained on the clinical research unit for subsequent Naltrexone treatment and PET imaging to determine the degree of mu and delta receptors blockade induced by Naltrexone (Weerts et al, 2008). HC subjects were admitted to the clinical research unit and completed the PET imaging followed the next day by the naloxone challenge prior to discharge.

The Clinical Institute Withdrawal Assessment-Alcohol Revised (CIWA-Ar) (Sullivan et al, 1989) was administered to the AD subjects 3 times each day for the first 5 days by the CRU nursing staff. Based on CIWA scores, vital signs and physician assessment, no subject required withdrawal medication during the inpatient protocol. Twenty of the 25 AD subjects and 2 of the HC subject were smokers. Cigarette smoking was prohibited for all subjects during the inpatient stay. To reduce the potential impact of nicotine withdrawal on outcomes, nicotine dependent subjects were provided a transdermal nicotine patch (21 mg nicotine) at the time of admission. Nicotine patches were applied daily until discharge.

PET procedures

PET images were obtained in 3D mode on a GE Advance PET scanner (GE Medical Systems, Milwaukee, WI) as described in detail previously (Weerts et al, 2011). Subjects completed two PET scans on the same day and in fixed order: a [11C]Methylnaltrindole scan, using a specific delta opioid receptor antagonist (Wand et al, In Press) and [11C]CFN scan using a specific mu opioid agonist (Frost et al, 1990; Titeler et al, 1989). Scans were conducted at 8:30 and 10:45 am, respectively. The current analysis only includes results from the [11C] CFN scan.

Prior to tracer injection a 10-minute transmission scan was completed. Following intravenous bolus administration of [11C]CFN (20.0±0.6 mCi SA: 21,482.7 ± 3310.1 mCi/ μmole for the HC group, and 19.3±0.5 mCi SA: 18,444.1 ± 2849.6 mCi/μmole for the AD group), 25 images with variable time intervals (6×30 sec, 5×60 sec, 5×120 sec, 9×480 sec) were acquired over 90-minutes. Specific activity measurements were made at the end of synthesis. The dose of carfentanil administered was less than 0.04 μg/kg body weight; no agonist effects were reported. Reconstruction of images was corrected for attenuation, scatter, and dead-time (Kinahan and Rogers, 1989). Each PET frame contained a $128 \times 128 \times 35$ matrix with voxel size of $2 \times 2 \times 4.25$ mm in a spatial resolution of 5.5 and 6.1 mm full-width-at-half-maximum (FWHM) in the radical and tangential directions, respectively, at 10 cm radius from the center of the field-of-view.

Volumes of Interest (VOI) Analyses

Fifteen VOIs were selected to include brain regions that had moderate to high [11C]CFN BP_{ND} and included regions that are altered in alcohol dependence (Weerts et al, 2011). The VOIs were defined as previously described (Weerts et al, 2011) and applied to PET frames to obtain time-activity curves (TACs) of regions.

PET Outcome Variables

[11C]CFN (BP_{ND}) was the primary dependent variable (Innis et al, 2007). BP_{ND} is derived from the product of the receptor density (Bmax' or the receptor density Bmax less those occupied by endogenous transmitters) and binding affinity (1/KD). Reference tissue graphical analysis (RTGA) (Logan et al, 1996) was employed with <u>occipital region</u> selected as the reference region. The brain-to-blood clearance rate constant of the reference region ($\overline{k_2}$) was set at a published population mean of 0.104 min^{-1} (Endres et al, 2003; Frost et al, 1990). There is a highly significant correlation between BP_{ND} estimates using RTGA and those obtained from the arterial input-based kinetic model (Endres et al, 2003).

Naloxone cumulative dosing procedure—A dose response curve to naloxone was generated for each subject and carried out in a single session based on our previously published procedures (Wand et al, 2011). Following a calorie controlled lunch at 1200 h participants had an intravenous catheter placed into a forearm vein 60 min before placebo administration. Baseline blood samples were drawn −30 min, −15 min and directly preceding placebo administration. The placebo (0.9% saline) was administered as a bolus at time 0. Incremental doses of naloxone (25, 50, 100 and, 250 ug/kg) dissolved in 0.9% saline were administered every 30 min. Blood draws took place 15 and 30 min after placebo and each naloxone dose, and then every 30 min through 240 min. Plasma cortisol (Diagnostic Products Corporation, Inc.; Los Angeles, CA) was assayed by radioimmunoassay. Intra-assay and inter-assay coefficients of variance were less than 8% for cortisol.

Statistical Plan—Multiple linear regression models were built to compare [11C]CFN BP between HC and AD group in 15 brain regions. Sex and current smoking status were added

as covariates. Adaptive step-up Bonferroni method was used for multiple comparison correction across brain regions (Hochberg and Benjamin, 1990).

Cortisol data was examined both as a function of time and dose of naloxone. To construct a naloxone dose response curve the cortisol value for each naloxone dose was calculated as the average of the two time points 15 minutes and 30 minutes after the dose was administered. Metrics based on the cortisol time series provided higher resolution for correlation analyses than the dose series and therefore were employed to examine the relationships between $[^{11}C]CFN$ (BP_{ND}) and cortisol metrics (see below). The baseline cortisol level was calculated as the average cortisol at −30, −15, and 0 minute. Mean cortisol curves were plotted to visualize hormone responses for HC and AD groups. To compare hormone levels following each dose of naloxone to baseline cortisol values, a linear mixed model with random intercept was constructed. An unstructured covariance matrix was used to obtain robust standard errors.

In a previous study we compared the relationship $[^{11}C]CFN$ (BP_{ND}) and area under the cortisol curve (AUC) in four brain regions of the HC subjects reported in this paper (Wand et al, 2011). For this study we tested three additional cortisol metrics to correlate with $[^{11}C]CFN$ (BP_{ND}): peak response, dose at peak response and the rising slope of the cortisol curve. This was done to see if we could identify a more robust cortisol metric that would correlate more strongly with $[^{11}C]CFN$ (BP_{ND}) and in more brain regions than AUC. The slope was calculated as the cortisol peak response (cortisol peak minus cortisol at 15 minute time point) divided by the duration from 15 minute to peak. Multi-linear model was constructed with BP_{ND} as the dependent variable and cortisol variables as the independent variable for each of the brain regions of interest

Sex and smoking modify naloxone-induced cortisol responses and $[^{11}C]CFN$ (BP_{ND}) (al'Absi et al., 2008; Uhart et al., 2006) and were added as covariates to the model. We also performed sensitivity analysis on age. There was not an association between age and $[^{11}C]CFN$ (BP_{ND}) in this data set, nor age changed the relationship between cortisol and BP for these models. Therefore age was not included in the final model. The p values were adjusted for multiple comparison correction across brain regions. The partial residual plots with the component line from the multi-linear models were plotted for selected regions to visualize correlation between the $[^{11}C]CFN$ (BP_{ND}) and cortisol slope after adjusting for sex and smoking status. $[^{11}C]CFN$ (BP_{ND}) was compared between HC and AD group using multi-linear regression, with sex and smoking status as covariates. All the analyses were carried out using SAS 9.3.

Results

We previously reported that $[^{11}C]CFN$ BP_{ND} was lower in the HC compared to AD subjects in the cingulate cortex, amygdala, insula, ventral striatum, putamen, caudate, globus pallidus, and thalamus (Weerts et al, 2011). In table 1 we compare $[^{11}C]CFN$ BP_{ND} in 7 additional brain regions not previously examined. We report that $[^{11}C]CFN$ BP_{ND} in these additional regions were lower in the HC compared to AD subjects.

The following day after the PET imaging procedure each subject underwent the naloxone challenge protocol. Baseline cortisol levels (mean of −30, −15 and 0 time points) did not differ by group. Compared to the effect of placebo, cumulative naloxone dose administration induced statistically significant cortisol responses in both HC and AD subjects (Figure 1). The mean naloxone dose required to produce the peak cortisol response was more than 2 times greater in AD compared to HC subjects (Table 2). The peak cortisol response and the slope of the rising cortisol curve were not statistically different by group.

We then examined the correlation between $[^{11}C]$CFN BP_{ND} and naloxone-induced cortisol response in all 15 brain regions using three cortisol metrics: rising slope, peak response and dose at peak response. There were significant negative correlations between the rising slope of the cortisol response curve and $[^{11}C]$CFN BP_{ND} in 9 of the 15 brain regions in the HC group (Table 3). The other cortisol metrics (dose at peak response and absolute peak response) did not correlate with $[^{11}C]$CFN BP_{ND} in HC subjects. In addition, there were no significant correlations between any naloxone-induced cortisol metric and $[^{11}C]$CFN BP_{ND} in AD subjects across the 15 brain region (Table 3).

As an example of these relationships, the partial residual plots show the association between $[^{11}C]$CFN BP_{ND} in the ventral striatum, caudate, putamen and hippocampus with cortisol rising slope in both groups after adjusted for sex and smoking (Figure 2A–H).

Discussion

In the current study we compared the relationship of $[^{11}C]$CFN BP_{ND} and cortisol responses to naloxone in HC and AD subjects. First we measured $[^{11}C]$CFN BP_{ND} in 15 brain regions in all subjects. We previously examined and reported on 8 regions finding lower $[^{11}C]$ CFN BP_{ND} in the HC group compared to AD subjects (Weerts et al, 2011). In the present study we compared $[^{11}C]$CFN BP_{ND} in HC and AD subjects measured in 7 additional brain regions that had not been previously reported. Again we found lower $[^{11}C]$CFN BP_{ND} in the HC group compared to AD subjects. The PET measurement in 7 additional brain regions indicates that elevated $[^{11}C]$CFN BP_{ND} in AD subjects is robust and more global than previously realized.

We then assessed cortisol responses to five incremental doses of naloxone. Although peak cortisol and cortisol slope did not differ between groups, there were group differences in the dose of naloxone required to achieve peak cortisol response. On average the AD subjects required twice the dose of naloxone to induce a peak cortisol response compared to the HC subjects. This observation is consistent with the PET findings of elevated $[^{11}C]$CFN BP_{ND} in AD subjects compared to HC subjects. The greater mu opioid receptor availability in AD subjects requires a higher dose of naloxone to block and maximally stimulate cortisol than lower mu opioid receptor availability in HC subjects.

We then proceeded to correlate $[^{11}C]$CFN BP_{ND} with three cortisol metrics. We previously reported in the HC subjects that there were significant negative relationships between cortisol AUC response to naloxone and $[^{11}C]$CFN BP_{ND} in ventral striatum, caudate, putamen and hypothalamus (Wand et al, 2011). For the present study we examined three other cortisol metrics attempting to find stronger correlations in many more brain regions. Based on this new data and our previous findings (Wand et al, 2011) it is clear that of the four cortisol metrics, the rising slope of the cortisol curve was the strongest predictor of $[^{11}C]$CFN BP_{ND} in the HC subjects.

The neurobiological mechanism(s) accounting for the correlation of naloxone-induced cortisol and $[^{11}C]$CFN BP_{ND} in the HC subjects is not clear. There are several possible explanations. Paraventricular CRF and AVP are the primary regulators of ACTH secretion, and thus cortisol. Opioid peptides inhibit the secretion of hypothalamic CRF (Boosook and Hyman 1995; Szekely, 1990). It is possible that the brains regions where $[^{11}C]$CFN BP_{ND} was found to correlate with cortisol are under mu opioid receptor inhibitory tone. The magnitude of naloxone-induced cortisol responses was proportional to mu receptor availability in these specific brain regions. The release of that inhibition by naloxone resulted in activating the hypothalamic regulators of ACTH through neural circuitry that connects each brain region with PVN neurons. Supporting this contention are preclinical

studies showing that mesolimbic brain regions that participate in responding to stressful stimuli also communicate with PVN neurons to stimulate CRF and AVP release or are involved in glucocorticoid negative feedback (Jankord and Herman, 2008). Therefore it is probably no coincidence that the correlation was identified mainly in mesolimbic brain regions.

Another potential mechanism underlying the correlation between cortisol and $[^{11}C]$CFN BP_{ND} may result from the effects of chronic cortisol exposure on mu opioid receptor expression. There is marked inter-individual variability in both stressed and non-stressed cortisol concentrations resulting from environmental and genetic influences (Stephens and Wand, In Press). Such inter-individual differences in the cortisol milieu could partially explain inter-individual differences in mu opioid receptor availability. Thus individuals with greater cortisol responses to life events may have lower mu opioid receptor availability compared to subjects with a more subdued stress response. In agreement with this premise is a PET study showing that sustained sadness as well as pain result in decreased $[^{11}C]$CFN BP_{ND} in the ventral basal ganglia, the nucleus accumbens, ventral pallidum, and in the amygdala (Ribeiro et al, 2005).

In contrast to the HC group, the AD subjects did not show correlations between their cortisol responses to naloxone and $[^{11}C]$CFN BP_{ND} in any of the 15 brain region. We also know that $[^{11}C]$CFN BP_{ND} and the dose of naloxone required to achieve peak cortisol responses were greater in AD subjects compared to HC subjects. These binding potential and neuroendocrine differences observed in the AD subjects may have resulted in the loss of correlation between mu opioid receptor availability and cortisol responses to naloxone. The cause of this interference may be secondary to alcohol toxicity or withdrawal. It is also plausible that these group differences preceded the development of significant alcohol exposure and were influenced by other environmental and/or genetic factors. The observation adds additional evidence that there is an important relationship between alcohol dependence, stress pathways and the endogenous opioid systems.

A possible weakness in the data is the potential confound of nicotine use which is so prevalent in HC subjects compared to social drinkers (Dawson, 2000). To minimize this potential confound smokers wore nicotine patches to minimize nicotine withdrawal. Additionally smoking was included as a covariate in the statistical model. Another weakness of the paper is the relatively small size which is typical for PET imaging studies. It should also be pointed out that we used a specific naloxone challenge procedure using a cumulative dosing method developed in our laboratory (Wand et al, 2011). It is unclear if similar observations could be identified if a simpler, single naloxone dose procedure was utilized. Finally, plasma naloxone levels were not determined. It is possible that differences between HCs and ADs in naloxone metabolism could account for part of the findings.

In summary, naloxone induced cortisol secretion imparts information about individual differences in mu opioid receptor availability throughout the mesolimbic system in HC subjects. Among the cortisol metrics studied, the rising slope of the cortisol curve correlates most strongly with $[^{11}C]$CFN BP_{ND} and should be the preferred metric in future studies. Overall these observations suggest there is endorphinergic neurocircuitry that connects mesolimbic stress pathways with the hypothalamic regulators of ACTH in healthy subjects. These pathways appear to be disrupted during early abstinence in AD subjects.

Acknowledgments

References

al'Absi M, Wittmers LE, Hatsukami D, Westra R. Blunted opiate modulation of hypothalamic-pituitary-adrenocortical activity in men and women who smoke. Psychosom Med. 2008; 70(8):928–935. [PubMed: 18799426]

Adinoff B, Krebaum SR, Chandler PA, Ye W, et al. Dissection of hypothalamic-pituitary-adrenal pathology in one-month abstinent alcohol-dependent men: Response to CRH and naloxone. Alcohol Clin Exp Res. 2005; 29:528–537. [PubMed: 15834217]

Borsook D, Hyman SE. Proenkephalin gene regulation in the neuroendocrine hypothalamus: A model of gene regulation in the CNS. Am J Physiol. 1995; 269:E393–E408. [PubMed: 7573416]

Bucholz KK, Cadoret R, Cloninger CR, Dinwiddie SH, et al. A new, semi-structured psychiatric interview for use in genetic linkage studies: a report on the reliability of the SSAGA. J Stud Alcohol. 1994; 55(2):149–158. [PubMed: 8189735]

Dawson DA. Drinking as a risk factor for sustained smoking. Drug Alcohol Depend. 2000; 59(3):235–249. [PubMed: 10812284]

Frost JJ, Mayberg HS, Sadzot B, Dannals RF, et al. Comparison of [11C]diprenorphine and [11C]carfentanil binding to opiate receptors in humans by positron emission tomography. J Cereb Blood Flow Metab. 1990; 10(4):484–492. [PubMed: 2161414]

Genazzani AR. Central deficiency in beta-endorphin in alcohol addicts. J Clin Endocrinol Met. 1982; 55:583–586.

Gianoulakis C. Characterization of the effects of acute ethanol administration on the release of beta–endorphin peptides by the rat hypothalamus. Eur J Pharmacol. 1990; 180:21–29. [PubMed: 2142093]

Heinz A, Reimold M, Wrase J, Hermann D, et al. Correlation of stable elevations in striatal mu-opioid receptor availability in detoxified alcoholic patients with alcohol craving: a positron emission tomography study using carbon 11-labeled carfentanil. Arch Gen Psych. 2005; 62(1):57–64.

Innis RB, Cunningham VJ, Delforge J, Fujita M, et al. Consensus nomenclature for in vivo imaging of reversibly binding radioligands. J Cereb Blood Flow Met. 2007; 27:1533–1539.

Jankord R, Herman JP. Limbic regulation of hypothalamo-pituitary-adrenocortical function during acute and chronic stress. Ann N Y Acad Sci. 2008; 148:64–73. [PubMed: 19120092]

Kinahan PE, Rogers JG. Analytic 3D image reconstruction using all detected events. IEEE Trans Nuc Sci. 1989; 36(1):964–968.

Kranzler HR, Edenberg HJ. Pharmacogenetics of alcohol and alcohol dependence treatment. Curr Pharm Des. 2010; 16(19):2141–2148. [PubMed: 20482509]

Leriche M, Méndez M. Ethanol exposure selectively alters beta-endorphin content but not [3H]-DAMGO binding in discrete regions of the rat brain. Neuropeptides. 2010; 44(1):9–16. [PubMed: 20031207]

Li XW, Li TK, Froehlich JC. Alcohol alters preproenkephalin mRNA content in the shell and core of the nucleus accumbens. Alcohol Clin Exp Res. 1996; 20:53–62.

Logan J, Fowler JS, Volkow ND, Wolf AP, et al. Graphical analysis of reversible radioligand binding from time-activity measurements applied to [N-11C-methyl]-(−)-cocaine PET studies in human subjects. J Cereb Blood Flow Met. 1990; 10(5):740–47.

McCaul M, Wand GS, Eisenberg T, Cheskin L, et al. Naltrexone alters the subjective and psychomotor effects of alcohol. Neuropsychopharmacology. 2000; 22:480–492. [PubMed: 10731623]

McCaul M, Wand GS, Stauffer R, Lee S, et al. Naltrexone dampens ethanol-induced cardiovascular and HPA axis activation. Neuropsychopharmacology. 2001; 25:537–547. [PubMed: 11557167]

Meltzer CC, Bryan RN, Holcomb HH, Kimball AW, et al. Anatomical localization for PET using MR imaging. J Comput Assist Tomogr. 1990; 14(3):418–426. [PubMed: 2335611]

Méndez M, Leriche M, Carlos Calva J. Acute ethanol administration transiently decreases [3H]-DAMGO binding to mu opioid receptors in the rat substantia nigra pars reticulata but not in the caudate-putamen. Neurosci Res. 2003; 47(2):153–160. [PubMed: 14512140]

O'Malley SS, Froehlich JC. Advances in the use of naltrexone: an integration of preclinical and clinical findings. Recent Dev Alcohol. 2003; 16:217–245. [PubMed: 12638640]

Oswald L, Wand G. Opioids and Alcohol. Physiol Behav. 2004; 81(2):339–358. [PubMed: 15159175]

Ribeiro SC, Kennedy SE, Smith YR, Stohler CS, et al. Interface of physical and emotional stress regulation through the endogenous opioid system and mu-opioid receptors. Prog Neuropsychopharmacol Biol Psychiatry. 2005; 29(8):1264–80. [PubMed: 16256255]

Sarkar DK, Kuhn P, Marano J, Chen C, et al. Alcohol exposure during the developmental period induces beta-endorphin neuronal death and causes alteration in the opioid control of stress axis function. Endocrinology. 2007; 148(6):2828–2834. [PubMed: 17347308]

Sinha R, O'Malley SS. Craving for alcohol: findings from the clinic and the laboratory. Alcohol Alcohol. 1999; 34(2):223–230. [PubMed: 10344782]

Sobell, LC.; Sobell, MB. Timeline followback: A technique for assessing self-reported alcohol consumption. In: Litten, RZ.; Allen, J., editors. Measuring alcohol consumption: Psychosocial and biological methods. Humana Press; New Jersey: 1992. p. 41-72.

Stephens, M.; Wand, G. Stress and Alcohol use disorders: the role of glucocorticoids. National Institutes of Health's Alcohol Health Research; 2011. In Press

Sullivan JT, Sykora K, Schneiderman J, Naranjo CA, et al. Assessment of alcohol withdrawal: the revised clinical institute withdrawal assessment for alcohol scale (CIWA-Ar). Brit J Addict. 1989; 84(11):1353–7. [PubMed: 2597811]

Swift RM, Whelihan W, Kuznetsov O. Naltrexone-induced alterations in human ethanol intoxication. Am J Psychiat. 1994; 151:1463–1467. [PubMed: 8092339]

Szekely JL. Opioid peptides and stress. Crit Rev Neurobiology. 1990; 6:1–12.

Titeler M, Lyon RA, Kuhar MJ, Frost JF, et al. Mu opiate receptors are selectively labelled by [3H]carfentanil in human and rat brain. Eur J Pharmacol. 1989; 167(2):221–228. [PubMed: 2556284]

Wand GS, Mangold D, Ali M. Adrenocorticotropin response to naloxone in sons of alcohol dependent men. J Clin Endocrinol Metabol. 1999; 84:64–68.

Wand GS, Mangold D, El Diery S, McCaul M, et al. Family history of alcoholism and hypothalamic opioidergic activity. Arch Gen Psychiat. 1998; 55:1114–1119. [PubMed: 9862555]

Wand G, Weerts E, Kuwabara H, Frost JJ, et al. Naloxone-induced cortisol predicts mu opioid receptor binding potential in specific brain regions. Psychoneuroendocrinology. 2011; 36(10):1453–1459. [PubMed: 21549509]

Wand G, Weerts E, Kuwabara H, Wong DF, et al. The Relationship between naloxone-induced cortisol and delta opioid receptor availability in mesolimbic structures is disrupted in alcohol dependent subjects. Addict Biol. 2012 In Press.

Weerts EM, Wand G, Kuwabara H, Munro CA, et al. PET imaging of mu- and delta-opioid receptor binding in alcohol dependent and healthy control subjects. Alcohol Clin Exp Res. 2011; 12:2162–2173. [PubMed: 21689118]

Weerts E, Kim Y, Wand G, Dannals R, et al. Differences in mu- and delta opioid receptor blockade measured by PET in Naltrexone-treated recently abstinent alcohol dependent subjects. Neuropsychopharmacology. 2008; 33(3):653–665. [PubMed: 17487229]
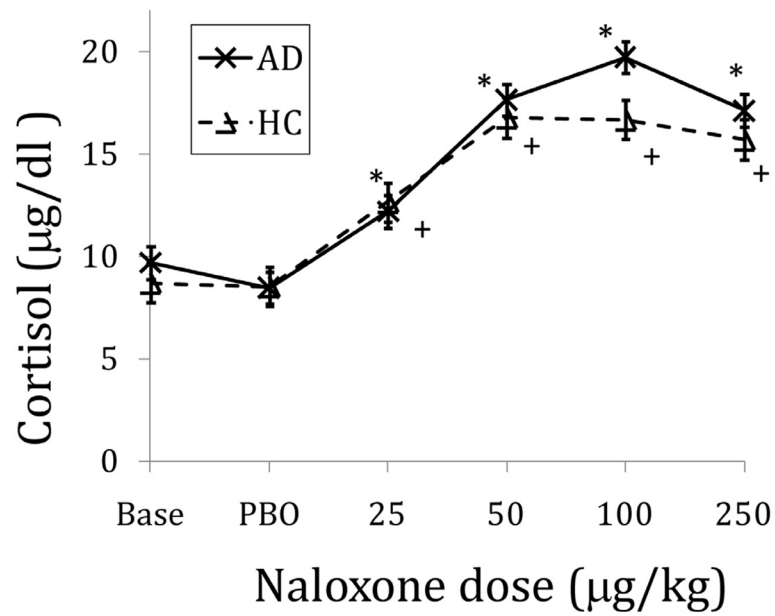
Figure 1.
Cortisol responses to five graded doses of naloxone, adjusted for sex and smoking. Data points are mean (SEM). BASE=baseline; PBO=placebo. * denotes time points in alcohol dependent subjects that were significantly different from mean of placebo time points with p<.05, adjusting for sex and smoking status. + denotes time points in healthy control subjects that were significantly different from mean of placebo time points with p<.05, adjusting for sex and smoking status.
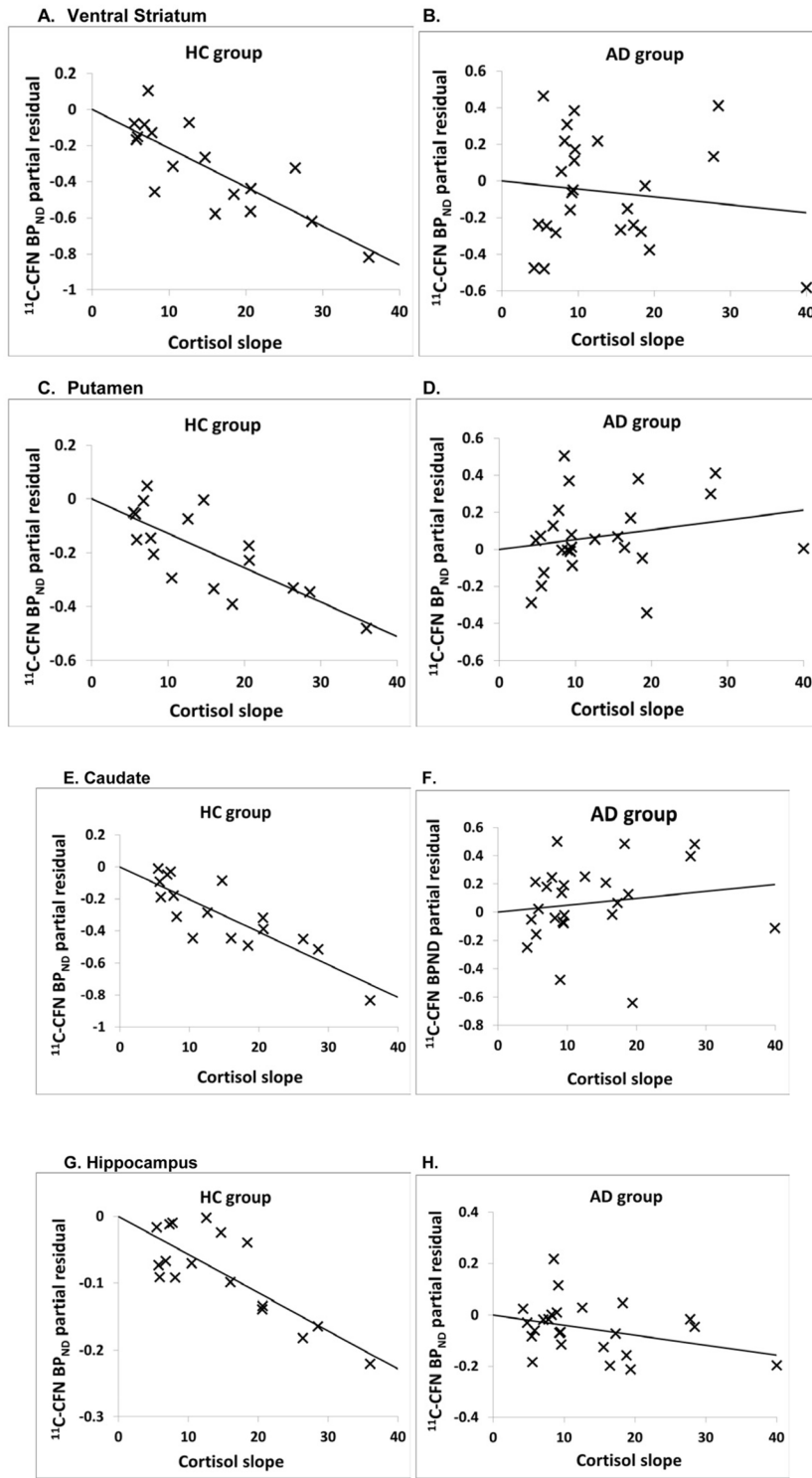
Figure 2.
Partial residual plots of [^{11}C]CFN BP$_{ND}$ and cortisol slope response adjusted for sex and smoking (for regression in table 3). Statistics are displayed in Table 4. A and B: ventral striatum; C and D: putamen; E and F: caudate; G and H: hippocampus.

Table 1

Mean ^{11}C-CFN BP of healthy control (HC) and alcohol dependent (AD) subjects. Data shown are group means and SEM adjusted for sex and smoking for each VOI.

VOI	HC (N = 18)	AD (N = 25)	Unadjusted P	Adjusted P
Fusiform	0.141 (0.02)	0.286 (0.017)	<0.001	<0.001
Temporal	0.501 (0.03)	0.665 (0.025)	<0.001	<0.001
Hypothalamus	1.031 (0.093)	1.34 (0.078)	0.028	0.028
Frontal Cortex	0.492 (0.032)	0.643 (0.027)	0.003	0.003
Hippocampus	0.122 (0.03)	0.232 (0.025)	0.015	0.015
Parietal	0.284 (0.022)	0.387 (0.018)	0.002	0.002
DLPFC[*]	0.376 (0.033)	0.481 (0.028)	0.036	0.036

[*]
dorsal lateral prefrontal cortex

Table 2

Comparisons of mean cortisol variables between healthy control (HC) and alcohol dependent (AD) subjects adjusted for smoking status and sex.

Variable	Adjusted mean (SE)		P
	HC (N = 18)	AD (N = 25)	
Peak (ug/dL)	21.0 (1.8)	23.6 (1.5)	0.332
Dose at peak (ug/kg)	65.7 (22)	144 (18.6)	0.019
Cortisol slope (30 min-peak)	15.5 (2.7)	12.9 (2.2)	0.560

Table 3

Correlation of cortisol slope to naloxone and ^{11}C-CFN BP adjusted by sex and smoking. The adaptive step-up Bonferroni method was used to adjust P values for multiple comparisons.

Region	HC (N = 18)			AD (N = 25)		
	Partial correlation coefficient	Unadjusted P	Adjusted P	Partial correlation coefficient	Unadjusted P	Adjusted P
Fusiform	−0.242	0.385	0.53	−0.05	0.821	0.989
Ventral Striatum	−0.77	<0.001	**0.002**	−0.125	0.57	0.989
Cingulate	−0.516	0.049	0.098	−0.146	0.508	0.989
Temporal	−0.598	0.019	**0.037**	−0.064	0.773	0.989
Putamen	−0.722	0.002	**0.005**	0.215	0.325	0.989
Hypothalamus	−0.242	0.386	0.53	−0.304	0.159	0.989
Thalamus	−0.773	<0.001	**0.001**	−0.042	0.849	0.989
Caudate	−0.818	<0.001	**<0.001**	0.15	0.496	0.989
Insula	−0.62	0.014	**0.027**	−0.003	0.989	0.989
Frontal Cortex	−0.525	0.044	0.089	0.038	0.864	0.989
Hippocampus	−0.766	0.001	**0.002**	−0.333	0.12	0.989
Globus Pallidus	−0.656	0.008	**0.016**	−0.132	0.549	0.989
Parietal	−0.524	0.045	0.09	0.08	0.718	0.989
Amygdala	−0.614	0.015	**0.03**	−0.163	0.458	0.989
DLPFC[*]	−0.176	0.53	0.53	0.064	0.771	0.989

[*] dorsal lateral prefrontal cortex; bolded values reached statistical significance